

Theoretical and experimental vibrational study of miconazole and its dimers with organic acids: Application to the IR characterization of its inclusion complexes with cyclodextrins

Valéry Barillaro^{a,*}, Georges Dive^{b,1}, Eric Ziémons^c, Pascal Bertholet^a,
Brigitte Evrard^a, Luc Delattre^a, Geraldine Piel^a

^a *Laboratory of Pharmaceutical Technology, Department of Pharmacy, University of Liege, CHU-Tour 4, Bât. B36, Avenue de l'Hôpital, 1, B-4000 Liège, Belgium*

^b *Center for Protein Engineering, Chemical Department, University of Liege, Bât B6, Allée de la Chimie, 3, B-4000 Liège, Belgium*

^c *Laboratory of Analytical Chemistry, Department of Pharmacy, University of Liege, CHU-Tour 4, Bât. B36, Avenue de l'Hôpital, 1, B-4000 Liège, Belgium*

Received 6 July 2007; received in revised form 22 August 2007; accepted 24 August 2007
Available online 4 September 2007

Abstract

The geometry, frequency and intensity of the vibrational bands of miconazole were derived from the density functional theory (DFT) calculations with the hybrid functional B3LYP and the 6-31G(d) basis set. Starting from the fully AM1 optimized geometries of miconazole/ β CD/acids complexes, the miconazole/acid dimers were reoptimized at the B3LYP/6-31G(d) level. Three acids were studied: maleic, fumaric and L-tartaric acids. To begin with the vibrational spectral data obtained from solid phase in mid FT-IR spectrum of miconazole and its dimers are assigned based on the results of the normal modes calculations. All the observed spectra and the calculated ones are found to be in good agreement. In a second step, theoretical results allowed the assignment of FT-IR spectrum for the miconazole/HP γ CD inclusion complex produced by supercritical carbon dioxide treatment and confirmed the inclusion of miconazole. The experimental spectra for the miconazole/HP γ CD/acids complexes prepared by supercritical carbon dioxide processing were also assigned using theoretical results. The results confirmed the presence of a genuine inclusion complex and also the interaction between miconazole and the acid.

© 2007 Elsevier B.V. All rights reserved.

Keywords: Miconazole; Molecular modeling; Density functional theory; Normal mode; Miconazole/acid dimer; Cyclodextrin inclusion complexes

1. Introduction

Miconazole (1-2-((2,4-dichlorophenyl)-2-(2,4-dichlorophenyl)-methoxy)ethyl)-1-imidazole) is an antifungal drug with poor water solubility. For many years, authors have studied its interactions with cyclodextrins (CDs), a family of cyclic oligosaccharides consisting of 6–8 D-glucopyranosyl units linked by $\alpha_{(1\rightarrow4)}$ -glycosylic bonds and presenting an apolar cavity. Depending on their shape, CDs can accommodate molecules inside their cavity to form inclusion compounds which modify

the physico-chemical properties of the guest as its water solubility (Frömming and Szejtli, 1994). So, CDs are mainly used as excipients which can enhance aqueous solubility of sparingly soluble drugs (Loftsson and Brewster, 1996).

Infrared spectroscopy is a standard tool for structural characterization of chemical entities. The infrared assignments of miconazole have not yet been reported. For large molecules, quantum chemical calculations predicting harmonic frequencies and spectral intensities are essential when interpreting experimental infrared spectra. In the theoretical prediction of molecular vibrational properties, density-functional theory (DFT) has been demonstrated to be a cost-effective alternative to conventional *ab initio* approaches, more efficient than Hartree–Fock approach and second-order Møller–Plesset perturbation theory (MP2) (Johnson et al., 1993; Scott and Radom,

* Corresponding author. Tel.: +32 4 366 43 01; fax: +32 4 366 43 02.

E-mail address: v.barillaro@gmail.com (V. Barillaro).

¹ Equal contributors to this study.

1996; Wong, 1996). The DFT calculations with the hybrid exchange-correlation functional B3LYP (Beecke's three parameters (B3) exchange in conjunction with the Lee–Yang–Parr's (LYP) correlation functional) have been proved to be very effective for vibrational studies on several systems (Giese and McNaughton, 2002; Fu et al., 2003; Arici et al., 2005).

In our previous paper (Barillaro et al., 2007), we investigated the molecular structures of the miconazole/CD/acids complexes using the semiempirical Austin Model 1 (AM1) method developed by Dewar et al. (1985). The fully optimized geometries and the energetic outcomes of the complexes were determined. The role of the acid during the complexation of miconazole into cyclodextrins has been evidenced.

In another paper, we have shown that, after supercritical processing and in presence of cyclodextrins and of acids, the miconazole infrared spectrum is modified (Barillaro et al., 2004). The aim of the present work is to compute the equilibrium geometry, vibrational frequencies and infrared intensities for miconazole and miconazole/acids dimers using hybrid DFT and medium basis set. These calculations enable the assignment of the bands in the experimental pellet infrared spectra for both miconazole and miconazole/acids dimers. Then, the miconazole/CD(acids) complexes infrared spectra were analyzed with the help of the theoretical results in order to point out interaction between the compounds and to confirm the presence of genuine inclusion complexes.

2. Materials and methods

2.1. Materials

Miconazole base ((1-2-((2,4-dichlorophenyl)-2-(2,4-dichlorophenyl)-methoxy)ethyl)-1-imidazole) was obtained from Janssen Pharmaceutica (Beerse, Belgium). Hydroxypropyl- γ -CD (HP γ CD) (Cavasol[®] W8 HP, MS 0.58, 1.62% H₂O) was obtained from Wacker Chemie GmbH (Munich, Germany). Fumaric acid was from Fluka (Buchs, Switzerland), maleic acid from Acros (New Jersey, USA) and L-tartaric acid (Eur Ph. 4th Edition) from Merck (Damstadt, Germany).

CO₂ was of N48 quality (99.998%) from Air Liquide (Liège, Belgium). All the products were used as received.

2.2. Methods

2.2.1. Preparation of the physical mixtures

All the physical mixtures were prepared by gently grinding, in a mortar, the calculated and exactly weighed amounts of compounds in equimolar ratio.

2.2.2. Experimental preparation of the miconazole/acid associations

The miconazole/acid associations were prepared as follow: the miconazole/acid physical mixtures were left in an oven at 125 °C for 60 min, these conditions simulating temperature conditions in the supercritical carbon dioxide experiments.

2.2.3. Experimental preparation of the inclusion compounds using supercritical carbon dioxide processing

The inclusion complexes were produced using supercritical carbon dioxide (SCCO₂) following a procedure and using an experimental set-up previously described (Barillaro et al., 2004). Miconazole/HP γ CD 1:1 (mol:mol) and miconazole/HP γ CD/acids 1:1:1 (mol:mol:mol) physical mixtures were processed by supercritical carbon dioxide in a static mode at 30 MPa, 125 °C during 60 min. At the end of the experiment, the vessel was depressurized within 15 s. The vessel content, in the form of a compact solid, was emptied, ground and homogenized in a mortar before further analysis.

2.2.4. FT-IR spectrum

The transmission IR spectra were recorded from isotopically dispersed products in KBr. The FT-IR spectra were collected over the spectral region 4000–600 cm⁻¹ at a resolution of 0.5 cm⁻¹ on a computer interfaced Bruker Tensor 27 FT-IR spectrophotometer equipped with a N₂-cooled MCT detector. The number of scans was 64.

2.2.5. Normal modes analysis

A fully unconstrained geometry optimisation was performed at the DFT level using the 6-31G(d) basis set and gradient techniques with the help of the Gaussian 98 software (Frisch et al., 1998). The DFT level is the B3LYP functional which uses the three-parameter functional of Beecke (Becke, 1988; Becke, 1993) and the exchange-correlation term of Lee–Yang–Parr (Lee et al., 1988). For all the studied systems, all the degrees of freedom are optimized thus requiring a significant amount of computational time.

Starting from the AM1 optimized geometries for the miconazole/ β CD/acid complexes (Barillaro et al., 2007), the β CD was removed and the DFT geometry optimizations were carried out without constraints. As two docking modes have been studied (dock1 and dock2), the B3LYP optimisations give rise to two different thermodynamically stable geometries for each miconazole/acid dimer.

To visualize the normal modes, the Molden[®] v. 3.5 software for Windows[®] was used (Schaftenaar and Noordik, 2000). For comparison with the experimental results, simulated IR spectra were calculated using the Swizard program revision 4.1 (Gorelsky, 2005) using the lorentzian model. The half-bandwidths ($\Delta 1/2, I$) were taken to be equal to 10 cm⁻¹. To facilitate the analysis of the results, only the mid wavenumber region (ca. 1700–1400 cm⁻¹) is considered.

3. Results

3.1. Normal modes analysis

Normal mode vibrational analyses at the B3LYP level were performed at the local energy minima characterized by all positive frequencies.

3.1.1. Miconazole

Miconazole is made of 39 atoms giving rise to 111 vibrational degrees of freedom. To allow the interpretation of the

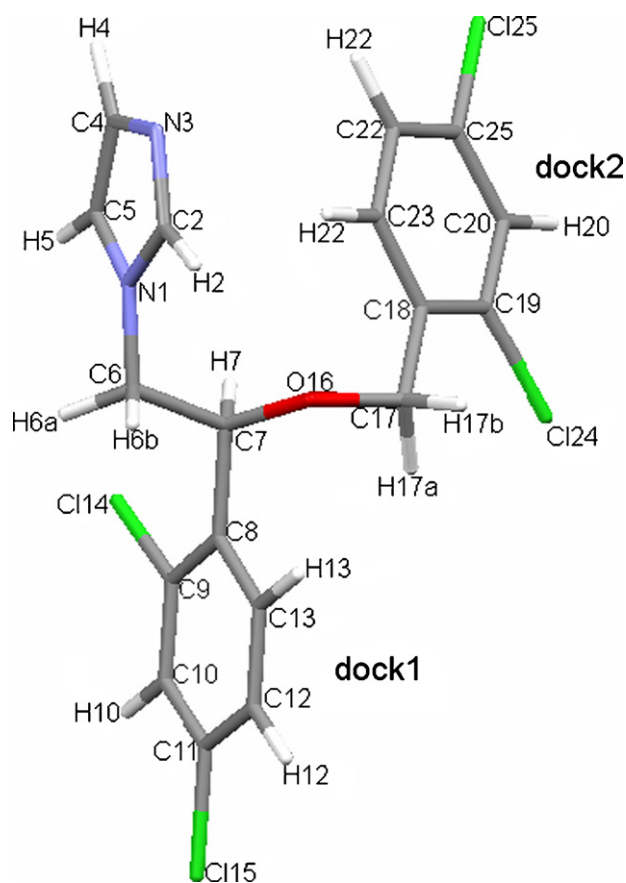


Fig. 1. B3LYP/6-31G(d) optimized geometry of miconazole.

experimental IR spectrum, harmonic vibrational frequencies, corresponding normal modes and IR intensities were calculated. For further agreements between computed and experimental frequencies, the computed frequencies can be scaled down with some specific factors (Scott and Radom, 1996; Wong, 1996). In this study, we chose to determine a scaling factor designed for miconazole. This calculated scaling factor 0.9711 is close to the one suggested by Scott and Radom (0.9614). To compare with the experimental results, a simulated IR spectrum was constructed as described above.

The B3LYP optimized geometry of miconazole is depicted in Fig. 1, the numbering of miconazole is made according to Blaton et al. (1978).

Comparison of the experimental and theoretical data shows that the FT-IR spectrum of miconazole very well reproduces the calculation (Fig. 2). In general, there is a one to one correspondence between the theoretically predicted and experimentally observed FT-IR bands. The relative intensities are also predicted quite well over the spectrum range.

In the mid-wavenumber region, four characteristic bands are observable (Table 1). The bands 1 and 2 at 1589 cm^{-1} and 1562 cm^{-1} respectively in the experimental spectrum are assigned to the CC stretching vibration of the two dichlorobenzene groups. The band 3 observed at 1510 cm^{-1} predicted at 1557.4 cm^{-1} and 1544.6 cm^{-1} corresponds to CC stretching vibration of the imidazole group as well as the CH bending of the imidazole group, the C6 of the aliphatic part of

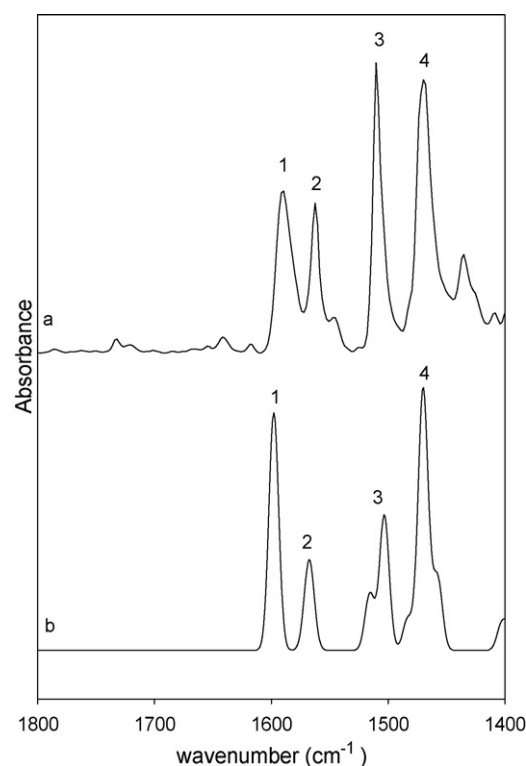


Fig. 2. Miconazole experimental spectrum (a) and B3LYP/6-31G(d) simulated spectrum (b) of the mid wavenumber region.

miconazole. The band 4 at 1470 cm^{-1} is the result of four theoretical vibrations predicted at 1523.9 cm^{-1} , 1511.2 cm^{-1} , 1508.6 cm^{-1} , 1497.8 cm^{-1} , corresponds to the CH bending of the two dichlorobenzene groups and to the CH bending of the C6 and C17.

Table 1

Experimental and B3LYP/6-31G(d) level computed vibrational frequencies (in cm^{-1}) of miconazole in the mid wavenumber region of the spectrum

Band	B3LYP		Exp.	Approximate description
	Calculated	Scaled ^a		
1	1642.3	1595.6	1589	CC stretching (dock1)
	1641.7	1595.0	1589	CC stretching (dock2)
2	1611.8	1565.9	1562	CC stretching (dock2 > dock1)
	1609.6	1563.8	1562	CC stretching (dock1 > dock2)
3	1557.4	1513.1	1510	CC stretching + CH bending (imidazole ring)
	1544.6	1500.6	1510	CH bending (imidazole ring and C6)
4	1523.9	1480.5	1470	CH bending (C17)
	1511.2	1468.2	1470	CH bending (dock1)
	1508.6	1465.7	1470	CH bending (dock2 and C17)
	1497.8	1455.2	1470	CH bending (C6)

^a Harmonic frequencies were scaled by 0.9711.

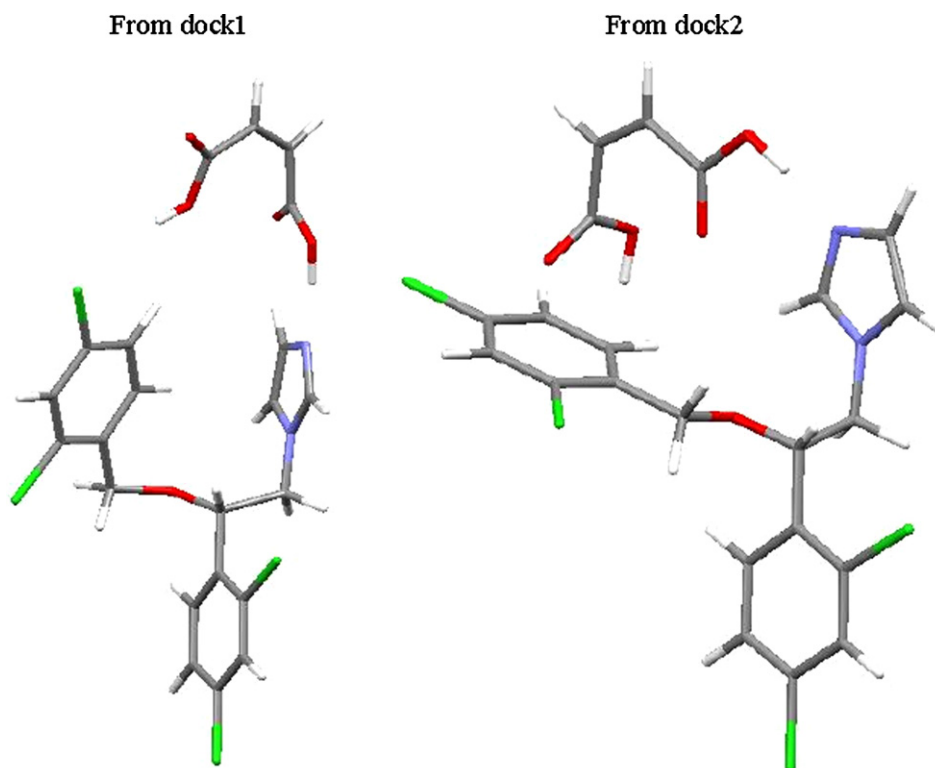


Fig. 3. B3LYP/6-31G(d) optimized geometries of miconazole/maleic acid associations calculated from both dock1 and dock2 inclusion modes.

3.1.2. Miconazole dimers

3.1.2.1. Miconazole/maleic acid. Starting from the optimized geometries of miconazole/ β CD/maleic acid complexes in both dock1 and dock2 inclusion modes (Barillaro et al., 2007), the optimization of the miconazole/maleic acid dimer at the B3LYP level of calculation was performed. This structure consisted in 51 atoms and gives rise to 147 degrees of freedom. The optimized geometries are shown in Fig. 3.

Obviously, as the starting points of the B3LYP optimization are not the same, the optimized geometries are also different. Strong interactions between miconazole and maleic acid occur in both conformations. Indeed, hydrogen bonds between miconazole and maleic acid can take place in order to stabilize the structures (Table 2).

Tables 3 and 4 compare the experimental and calculated theoretical frequencies. The experimental assignment is given in terms of chemical group fragments motions. For visual comparison, the observed and the calculated FT-IR spectra of miconazole/maleic acid dimers in the mid-wavenumber region is depicted in Fig. 4.

Table 2

Interatomic distances (\AA) between some function of miconazole and maleic acid able to form hydrogen bounds

Miconazole/maleic acid	Miconazole	Maleic acid	Distance (\AA)
From dock1	N3	OH	1.728
	CH22	OH	2.689
From dock2	N3	OH	1.695
	CH22	C=O	2.336
	CH22	C=O	2.317

Close inspection of Tables 3 and 4 shows that agreement between measured peak position and their theoretically calculated counterparts is generally good. Most bands lie within $5\text{--}10\text{ cm}^{-1}$ of predicted values, some within 20 cm^{-1} and only few differ by as much as 30 cm^{-1} . However, as it can be seen in Fig. 4, the variation between the measured and the calculated band intensities are significantly larger. Despite this, the over-

Table 3

Experimental and B3LYP/6-31G(d) level computed vibrational frequencies (in cm^{-1}) of miconazole/maleic acid dimer from dock1 in the mid wavenumber region of the spectrum

Band	B3LYP		Exp.	Approximate description
	Calculated	Scaled ^a		
1	1822.9	1770.6	1707	C=O stretching
	1797.4	1745.8	1707	C=O stretching
	1705.7	1656.7	1617	C=C stretching
2	1641.7	1594.6	1590	CC stretching (dock2)
	1641.6	1594.5	1590	CC stretching (dock1)
3	1612.8	1566.5	1564	CC stretching (dock2)
	1610.2	1564.0	1564	CC stretching (dock1)
4	1571.2	1526.1		CC stretching (imidazole ring)
	1554.6	1510.0	1508	CH bending (imidazole ring)
5	1525.0	1481.2	1473	CH bending (C17)
	1512.4	1469.0	1473	CH bending (dock2 and C17)
	1511.5	1468.1	1473	CH bending (dock1, C17 and C7)
	1504.3	1461.1		OH bending
6	1498.7	1455.7		CH bending (C6)

^a Harmonic frequencies were scaled by 0.9711, in *italic*: normal modes of maleic acid.

Table 4

Experimental and B3LYP/6-31G(d) level computed vibrational frequencies (in cm^{-1}) of miconazole/maleic acid dimer from dock2 in the mid wavenumber region of the spectrum

Band	B3LYP		Exp.	Approximate description
	Calculated	Scaled ^a		
	1832.0	1779.4	1707	<i>C=O stretching</i>
	1771.3	1720.5	1707	<i>C=O stretching</i>
	1718.5	1669.2	1617	<i>C=C stretching</i>
1	1644.0	1596.8	1590	CC stretching (dock2)
	1642.1	1595.0	1590	CC stretching (dock1)
2	1613.0	1566.7	1564	CC stretching (dock2)
	1610.2	1564.0	1564	CC stretching (dock1)
3	1570.8	1525.7		CC stretching (imidazole ring)
	1555.4	1510.8	1508	CH bending (imidazole ring)
4	1533.9	1489.9	1473	CH bending (C17)
	1521.7	1478.0	1473	<i>Bending OH</i>
	1514.9	1471.4	1473	CH bending (dock2)
	1511.3	1467.9	1473	CH bending (dock1 and C17)
	1498.7	1455.7	1473	CH bending (C6)

^a Harmonic frequencies were scaled by 0.9711, in *italic: normal modes of maleic acid*.

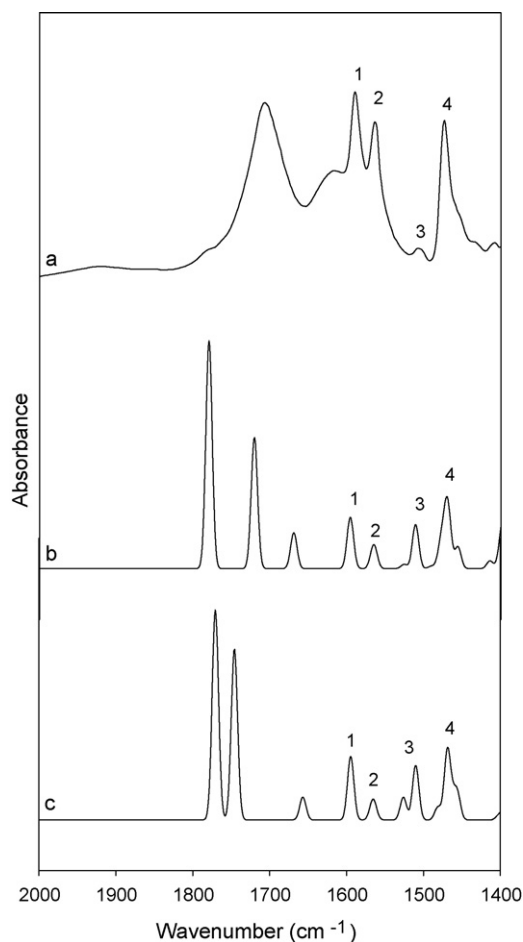


Fig. 4. Expansion of the FT-IR spectra for miconazole/maleic acid systems: experimental spectrum (a); B3LYP/6-31G(d) theoretical spectra for the dimer from dock2 (b) and from dock1 (c).

all agreement between the theory and the experiment is good and the calculated normal modes provide valuable insight into molecular characteristics.

Comparison of the spectrum of miconazole with those of miconazole/maleic acid dimers reveals that the presence of this acid does not modify the miconazole spectrum. According to the B3LYP calculations performed on dimers, the portion of the spectrum resulting of miconazole vibration is the same for both dimers. The FT-IR bands 1 and 2 at 1590 cm^{-1} and 1564 cm^{-1} are assigned to CC stretching for dock1 and dock2. The FT-IR band 3 observed at 1508 cm^{-1} is due to imidazole CH bending. The band 4 observed at 1473 cm^{-1} is the result of several vibrations: CH bending of dock1, dock2, C6 and C17 and also OH bending (maleic acid).

In the experimental spectrum, a large band is observed at 1707 cm^{-1} and is due to the shoulder of several theoretical bands: two bands of C=O stretching predicted between 1780 cm^{-1} and 1720 cm^{-1} and also the CC stretching of maleic acid predicted between 1650 cm^{-1} and 1670 cm^{-1} depending on the dimer conformation. This large experimental band is thus characteristic of the interaction between miconazole and maleic acid. It is interesting to note that both optimized geometries, starting point for the vibrational frequencies calculation, represent two thermodynamically stable geometries in gas phase. Nevertheless, in solid state, several other geometries can occur. This is the reason why the band experimentally observed at 1707 cm^{-1} is wider than those observed in the theoretical ones. This observation can be made for all the studied dimers.

3.1.2.2. Miconazole/fumaric acid. The structures of the miconazole/fumaric acid dimer reoptimized from the inclusion complex with βCD (in the dock1 and dock2 modes) are depicted in Fig. 5. These structures consisted in 51 atoms giving rise to 147 degrees of freedom. As observed for the first miconazole/acid association, the two different starting points give rise to two optimized geometries. Table 5 shows that the formation of hydrogen bonds takes place between miconazole and fumaric acid to stabilize the association.

Tables 6 and 7 present the calculated vibrational frequencies for the miconazole/fumaric acid dimers reoptimized from the dock1 and the dock2 complexes with βCD respectively. Each of these tables gives the experimentally reported infrared frequencies of the molecules for comparison. Each vibrational mode was assigned to some types of motion. The assignment of each

Table 5

Interatomic distances (\AA) between some function of miconazole and fumaric acid able to form hydrogen bonds

Miconazole/fumaric acid	Miconazole	Fumaric acid	Distance (\AA)
From dock1	N3	OH	1.718
	CH2	C=O	2.350
From dock2	N3	OH	1.712
	CH2	C=O	2.315
	CH23	C=O	2.579

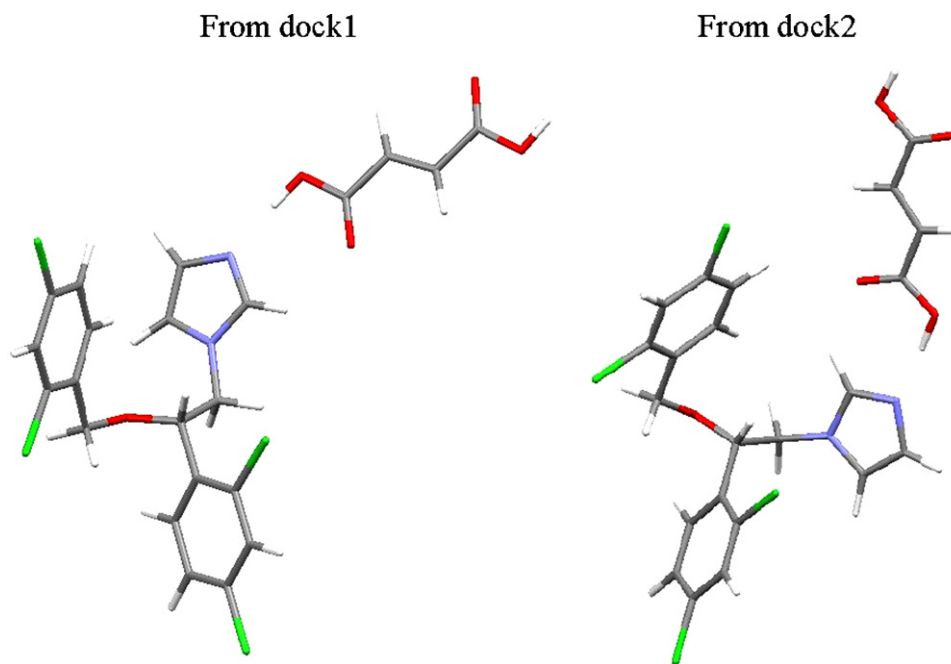


Fig. 5. B3LYP/6-31G(d) optimized geometries of miconazole/fumaric acid associations calculated from both dock1 and dock2 inclusion modes.

normal mode is also given in each table. Comparing the results of Tables 6 and 7 with the experimental values reflects an excellent agreement for the vibrational frequencies. The calculated and experimental spectra of miconazole/fumaric acid dimers are shown in Fig. 6.

As observed for the miconazole/maleic acid dimer, the four characteristic bands of miconazole are not so modified by the

Table 6
Experimental and B3LYP/6-31G(d) level computed vibrational frequencies (in cm^{-1}) of miconazole/fumaric acid dimer from dock1 in the mid wavenumber region of the spectrum

Band	B3LYP		Exp.	Approximate description
	Calculated	Scaled ^a		
	1827.1	1774.7	1694	<i>C=O stretching free</i>
	1783.1	1731.9	1675	<i>C=O stretching bound</i>
	1730.3	1680.6		<i>CC stretching</i>
1	1643.4	1596.3	1589	CC stretching (dock2)
	1640.9	1593.8	1589	CC stretching (dock1)
2	1612.8	1566.5	1563	CC stretching (dock2)
	1610.2	1564.0	1563	CC stretching (dock1)
3	1568.6	1523.6	1524	CC stretching (cycle imidazole)
	1550.0	1505.5	1507	CH bending (imidazole ring and C6)
4	1522.3	1478.6	1467	CH bending (C17)
	1511.6	1468.2	1467	CH bending (dock1)
	1510.7	1467.4	1467	<i>OH bending free</i>
	1508.6	1465.3	1467	CH bending (dock2)
	1497.1	1454.2	1467	CH bending (C6)
	1443.9	1402.5	1434	CH bending (C6 et C17)
	1435.6	1394.4	1434	CH bending (C6 et C17)
	1426.7	1385.8	1434	CH bending (dock1 and C7)
	1416.6	1375.9	1434	CH bending (C6)

^a Harmonic frequencies were scaled by 0.9711, in *italic*: normal modes of fumaric acid.

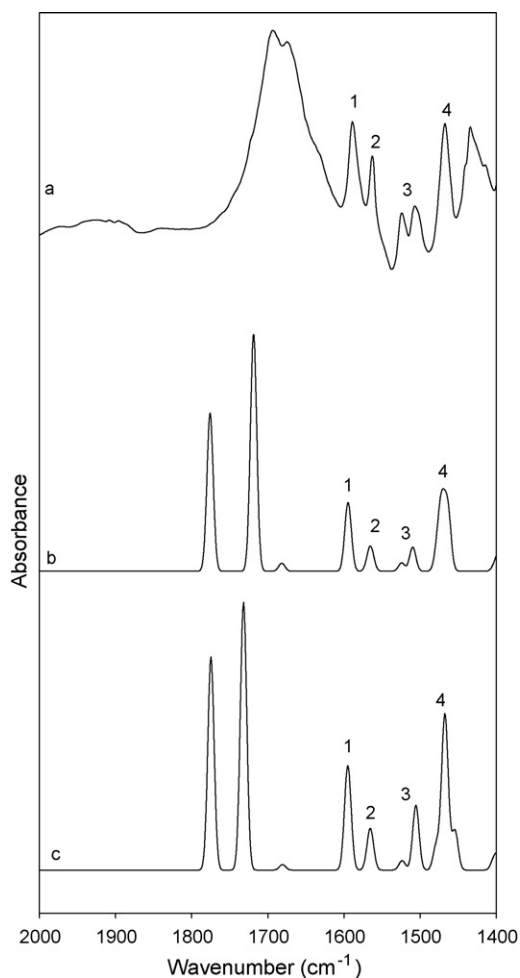


Fig. 6. Expansion of the FT-IR spectra for miconazole/fumaric acid systems: experimental spectrum (a); B3LYP/6-31G(d) theoretical spectra for the dimer from dock2 (b) and from dock1 (c).

Table 7

Experimental and B3LYP/6-31G(d) level computed vibrational frequencies (in cm^{-1}) of miconazole/fumaric acid dimer from dock2 in the mid wavenumber region of the spectrum

Band	B3LYP		Exp.	Approximate description
	Calculated	Scaled ^a		
	1828.3	1775.8	1694	<i>C=O stretching free</i>
	1769.5	1718.7	1675	<i>C=O stretching bound</i>
	1731.27	1681.6		<i>C=C stretching</i>
1	1643.07	1595.9	1589	CC stretching (dock2)
	1640.85	1593.8	1589	CC stretching (dock1)
2	1612.87	1566.6	1563	CC stretching (dock2)
	1609.8	1563.6	1563	CC stretching (dock1)
3	1569.29	1524.3	1524	CC stretching (imidazole ring)
	1554.22	1509.6	1507	CH bending (imidazole ring and C6)
4	1520.72	1477.1	1467	CH bending (C17)
	1514.99	1471.5	1467	CH bending (dock1)
	1508.69	1465.4	1467	CH bending (C6)
	1507.14	1463.9	1467	CH bending (C17)
	1505.16	1462.0	1467	<i>OH bending (bound)</i>
	1442.48	1401.1	1434	CH bending (C6 and C17)

^a Harmonic frequencies were scaled by 0.9711, in *italic*: normal modes of fumaric acid.

presence of the fumaric acid. The major difference is the band 3 which splits into two bands: the first one is assigned to the CC stretching of the imidazole ring and the second one to the CH bending of the C6 and of the imidazole ring.

Table 8

Interatomic distances (\AA) between some function of miconazole and L-tartaric acid able to form hydrogen bonds

Miconazole/L-tartaric acid	Miconazole	L-Tartaric acid	Distance (\AA)
From dock1	N3	OH alc ^a	1.777
	CH22	OH alc ^a	2.357
	CH2	C=O	2.357
From dock2	N3	OH carb	2.604
	CH2	C=O ^a	2.189
	CH22	C=O ^a	2.423
	CH22	OH alc	2.600

^a Same function.

Once again, the C=O and CC stretchings of fumaric acid are observed in the experimental spectrum in a large band presenting two peaks at 1694 and 1675 cm^{-1} . This large band is thus characteristic of miconazole/fumaric acid interaction.

3.1.2.3. Miconazole/L-tartaric acid. These structures consisted in 55 atoms giving rise to 159 degrees of freedom. As observed for the others miconazole dimers, the calculated geometries are different because they are optimized from different geometries in the inclusion complexes with β CD (dock1 and dock2 modes). The structures are depicted in Fig. 7. As presented in Table 8, L-tartaric acid forms hydrogen bonds with miconazole which stabilize the complex.

The vibrational frequencies and approximate description of each normal modes obtained using the B3LYP method are given

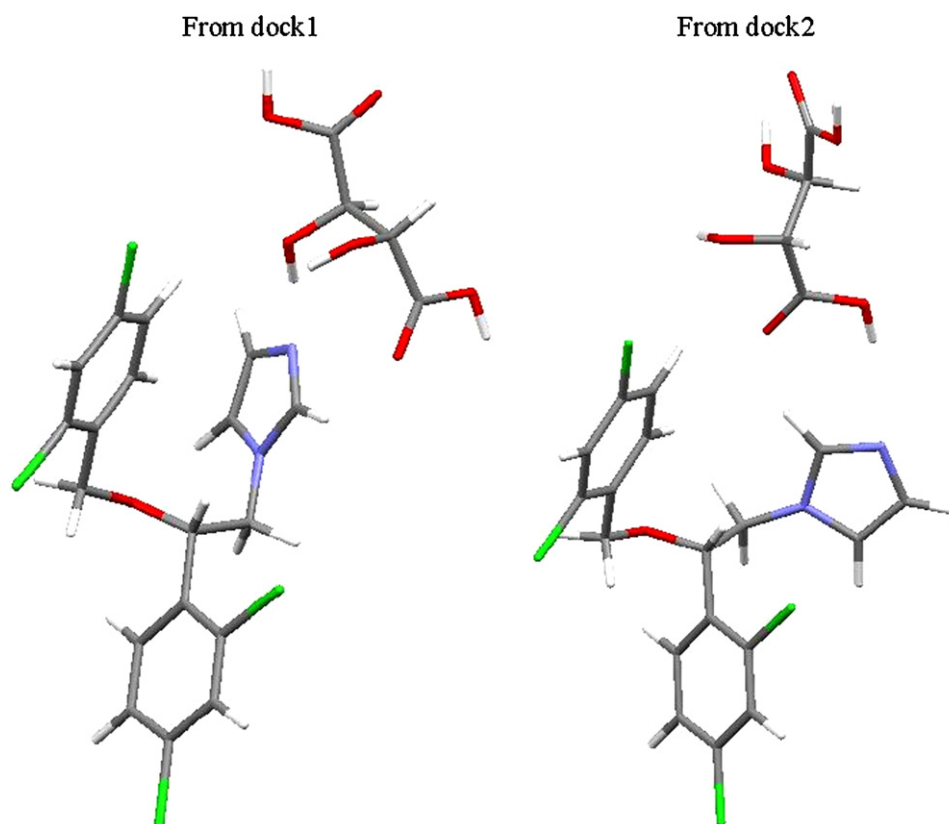


Fig. 7. B3LYP/6-31G(d) optimized geometries of miconazole/L-tartaric acid associations calculated from both dock1 and dock2 inclusion modes.

Table 9

Experimental and B3LYP/6-31G(d) level computed vibrational frequencies (in cm^{-1}) of miconazole/tartaric acid dimer from dock1 in the mid wavenumber region of the spectrum

B3LYP		Exp.	Assignment approximative
Calculated	Scaled		
1842.7	1789.8	1736	<i>C=O stretching</i>
1837.1	1784.4	1736	<i>C=O stretching</i>
1641.5	1594.4		CC stretching (dock2)
1641.3	1594.2		CC stretching (dock1)
1611.3	1565.1		CC stretching (dock2)
1609.3	1563.1		CC stretching (dock1)
1564.6	1519.7		CC stretching (cycle imidazole)
1553.8	1509.2		CH bending (cycle imidazole et C6)
1525.0	1481.2		CH bending (C17)
1514.4	1470.9		CH bending (dock2 and C17); <i>OH alc bending</i>
1511.3	1467.9		CH bending (dock1)
1499.1	1456.0		CH bending (C6)
1458.0	1416.1		<i>OH alc bending</i>
1443.5	1402.0		CH bending (dock2, C6 et C7)
1436.6	1395.3		CH bending (C6 et C7)

^aHarmonic frequencies were scaled by 0.9711, *in italic: normal modes of L-tartaric acid.*

in Tables 9 and 10. For visual comparison, the observed and the calculated (simulated) FT-IR spectra of miconazole/L-tartaric acid association in the mid-wavenumber region is depicted in Fig. 8.

It is very difficult to assign the experimental spectrum for the miconazole/L-tartaric acid dimer. Indeed, the characteristic bands of miconazole are not observable. Only one large band appears on the spectrum. Nevertheless, another large band at 1736 cm^{-1} is detected. This band is assigned to C=O stretching calculated at 1789.8 cm^{-1} and 1784.4 cm^{-1} .

Table 10

Experimental and B3LYP/6-31G(d) level computed vibrational frequencies (in cm^{-1}) of miconazole/tartaric acid dimer from dock2 in the mid wavenumber region of the spectrum

B3LYP		Exp.	Assignment approximative
Calculated	Scaled		
1842.9	1790.0	1736	<i>C=O stretching (free)</i>
1772.9	1722.0	1736	<i>C=O stretching (bound)</i>
1642.2	1595.0		Stretching CC (dock2)
1641.8	1594.7		Stretching CC (dock1)
1611.3	1565.0		Stretching CC (dock2)
1609.9	1563.7		Stretching CC (dock1)
1575.0	1529.8		Stretching CC (cycle imidazole); <i>OH carb bending (bounded)</i>
1558.2	1513.5		CH bending (cycle imidazole and C6); <i>OH carb. bending (bound)</i>
1542.0	1497.8		<i>OH carb bending (bounded); OH alc. bending</i>
1529.5	1485.6		CH bending (C17)
1517.3	1473.7		CH bending (dock2 et C17); <i>OH alc bending</i>
1511.3	1467.9		CH bending (dock1)
1499.8	1456.7		CH bending (C6)
1479.4	1436.9		<i>OH alc. bending</i>

^aHarmonic frequencies were scaled by 0.9711, *in italic: normal modes of L-tartaric acid.*

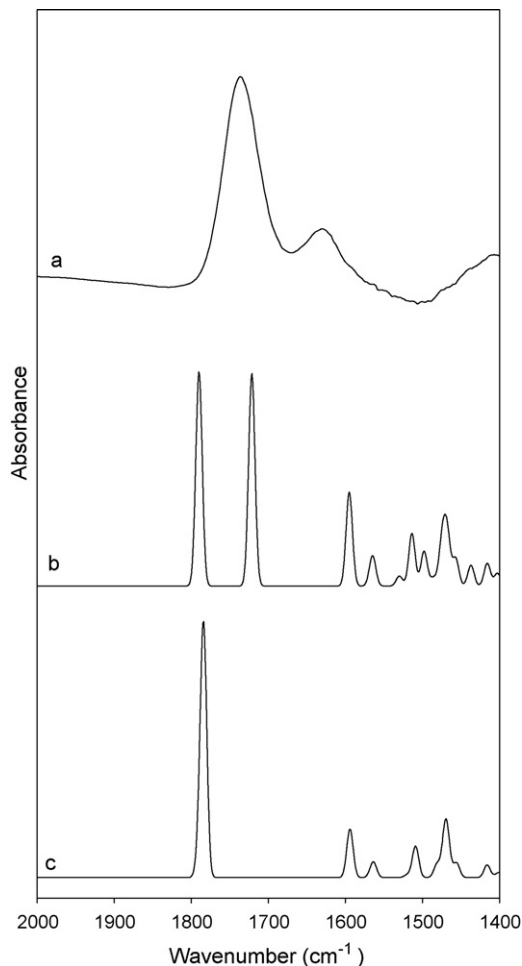


Fig. 8. Expansion of the FT-IR spectra for miconazole/L-tartaric acid systems: experimental spectrum (a); B3LYP/6-31G(d) theoretical spectra for the dimer from dock2 (b) and from dock1 (c).

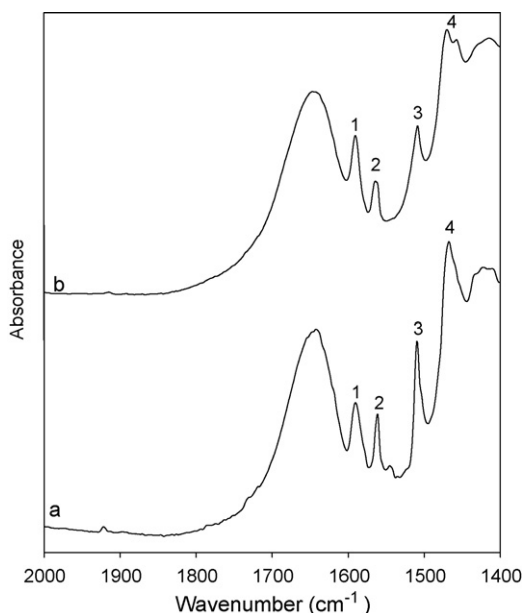


Fig. 9. Expansion of FT-IR experimental spectrum for miconazole/HP γ CD: physical mixture (a) and complex produced by supercritical fluids (b).

Table 11
Characteristic FT-IR bands positions of miconazole in miconazole/HP γ CD systems

Band	Physical mixture	SCCO ₂ complex
OH bending	1642	1647
1	1590	1590
2	1562	1564
3	1510	1509
4	1468	1470 and 1457

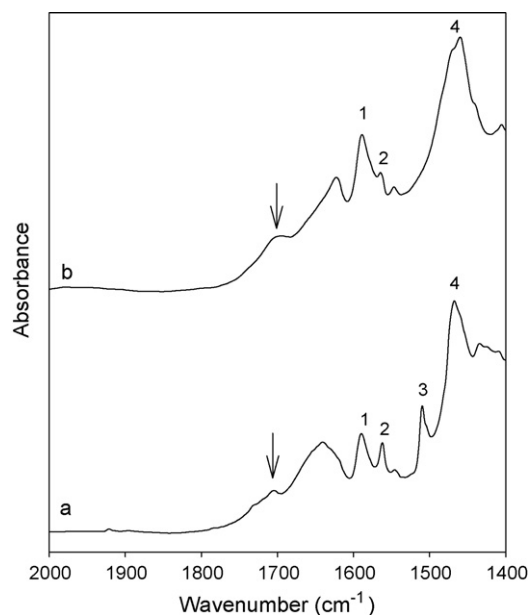


Fig. 10. Expansion of FT-IR experimental spectra for miconazole/HP γ CD/maleic acid: physical mixture (a) and complex produced by supercritical fluids (b).

3.2. FT-IR analysis of miconazole/cyclodextrin complexes

Once the miconazole and miconazole/acid dimers spectra assigned, the FT-IR spectra of miconazole/cyclodextrins/acid complexes can accurately be analyzed in order to confirm the miconazole inclusion and the interaction between miconazole and the acids. As explained in Section 2, the inclusion complexes were formed using supercritical carbon dioxide process.

3.2.1. Miconazole/HP γ CD complex

The spectra for the miconazole/HP γ CD complex and for the physical mixture are depicted in Fig. 9. In the spectra, a large

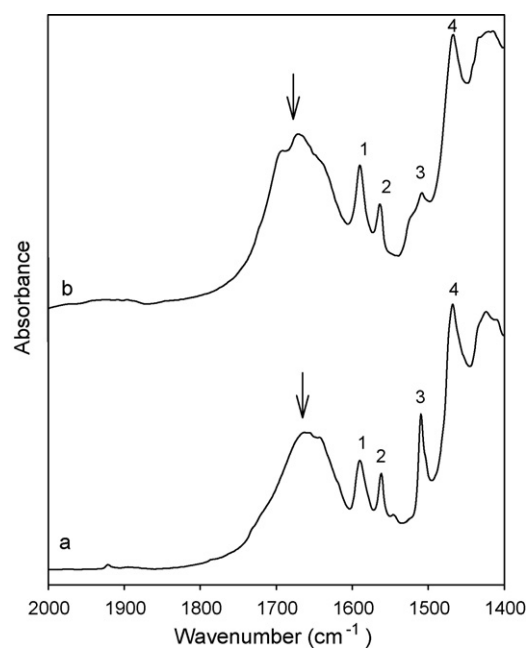


Fig. 11. Expansion of FT-IR experimental spectra for miconazole/HP γ CD/fumaric acid: physical mixture (a) and complex produced by supercritical fluids (b).

band around 1645 cm^{-1} is observed and is due to OH bending (cyclodextrin OH groups and water contained in the sample). The four bands characteristic of miconazole are observed. Upon complexation, some spectral modifications are detectable. As seen in Table 11, there are shifts and intensities modifications of miconazole bands. As determined with the B3LYP calculations, these modifications affect the two dichlorophenyl rings (dock1 and dock2) and the imidazole ring. It was previously demonstrated with the help of molecular modeling and ¹H-NMR spectroscopy that these parts of miconazole can interact with the cyclodextrin cavity (Barillaro et al., 2007; Piel et al., 2001a; Piel et al., 2001b). The inclusion of miconazole is confirmed at the solid state.

3.2.2. Miconazole/HP γ CD/acids complex

Three ternary complexes have been studied: miconazole/HP γ CD with maleic, fumaric and L-tartaric acid. The spectra are depicted in Figs. 10–12. Table 12 presents the most important FT-IR bands observed in the experimental spectra of the physical mixture and complex. It can be observed that in all

Table 12
Characteristic FT-IR bands positions of miconazole in miconazole/HP γ CD/acids systems

Band	Miconazole/HP γ CD/maleic acid		Miconazole/HP γ CD/fumaric acid		Miconazole/HP γ CD/L-tartaric acid	
	Physical mixture	SCCO ₂ complex	Physical mixture	SCCO ₂ complex	Physical mixture	SCCO ₂ complex
C=O	1706	1704	1661	1696 and 1671		1735
OH bending	^a	^a	^a	^a	1647	1642
1	1589	1589	1590	1590	1590	1590
2	1562	1564	1562	1563	1562	1562
3	1510	^a	1510	1509	1510	^a
4	1468	1460	1469	1469	1468	1549

^a Not observable.

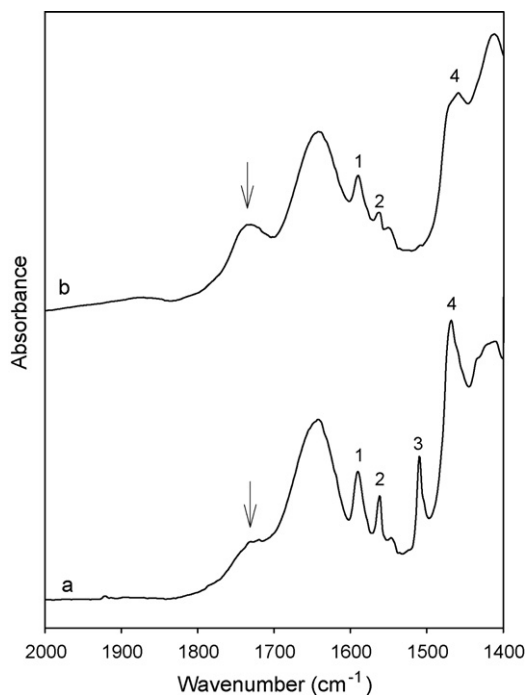


Fig. 12. Expansion of FT-IR experimental spectra for miconazole/HP γ CD/L-tartaric acid: physical mixture (a) and complex produced by supercritical fluids (b).

complexes, by comparison with the physical mixture, there are modifications of the four bands characteristic of miconazole: shift and decrease of intensity. As explained for the previous complex, the modifications of the bands assigned to the aromatic parts of miconazole molecule confirm the inclusion of miconazole into the HP γ CD cavity. Moreover, in all systems, the intensity of bands assigned to C=O stretching significantly increase in the complex spectra. As observed earlier, B3LYP calculations revealed that miconazole and the acid interact by means of the formation of hydrogen bonds. The analysis of the theoretical infrared spectra of the miconazole dimers showed that the 'miconazole' part of the spectrum is not modified but that the acid gives rise to high intensity bands between 1750 cm^{-1} and 1690 cm^{-1} . As it can be observed in Figs. 10–12, the intensity of the band due to the acid is weaker in the physical mixtures spectra than in the complex spectra. Thus, this increase of the intensity reflects the interaction between miconazole and the acid which establishes during the complexation.

4. Conclusions

DFT calculations at the B3LYP/6-31G(d) level were carried out on the structures and the vibrational spectra of miconazole and its dimers with maleic, fumaric and L-tartaric acids. A high level of conformity was found between experimental and scaled B3LYP frequencies which allow the accurate assignment of miconazole and of miconazole/acids dimers infrared spectra. The infrared bands characteristic of miconazole were determined. The results show that some modifications of these bands occur during complexation. It was demonstrated that these modifications affect the aromatic parts of miconazole, confirm-

ing the inclusion at the solid state. Moreover, in the ternary systems, the interaction between miconazole and the acid could be observed in the infrared spectra and revealed the presence of ternary complexes. These observations evidenced that the supercritical carbon dioxide processing enable the production of genuine binary and ternary miconazole/CD/(acid) inclusion complexes.

Eventually, the DFT calculations at the B3LYP/6-31G(d) level seem to be a very powerful tool for the characterization and the interpretation of infrared spectra of large molecules such as miconazole and its dimers with acids and allow to understand and describe the phenomena observed in larger systems such as cyclodextrins inclusion complexes.

Acknowledgments

This work was supported in part by the Belgian program on Interuniversity Poles of Attraction initiated by the Belgian State, Prime Minister's Office, Services fédéraux des affaires scientifiques, techniques et culturelles (PAI n° P4/03), the Fonds de la Recherche Scientifique Médicale Belge (FRSM, contrat n°3.4531.92).

This work was also funded in part by grants from the Fonds National de la Recherche Scientifique (Brussels, Belgium) (3.4.510.04.F).

Geraldine Piel is a scientific research worker supported by the Fonds National de la Recherche Scientifique.

Georges Dive is a research associate of the Fonds National de la Recherche Scientifique.

References

- Arici, K., Yurdakul, M., Yurdakul, S., 2005. HF and DFT studies of the structure and vibrational spectra of 8-hydroxyquinoline and its mercury(II) halide complexes. *Spectrosc. Acta Pt A-Molec. Biomolec. Spectr.* 61, 37–43.
- Barillaro, V., Bertholet, P., Henry de Hassonville, S., Ziémons, E., Evrard, B., Delattre, L., Piel, G., 2004. Effect of acidic ternary compounds on the formation of miconazole/cyclodextrin inclusion complexes by means of supercritical carbon dioxide. *J. Pharm. Pharm. Sci.* 7, 378–388.
- Barillaro, V., Dive, G., Bertholet, P., Evrard, B., Delattre, L., Ziémons, E., Piel, G., 2007. Theoretical and Experimental investigations on miconazole/cyclodextrin/acid complexes: molecular modeling studies. *Int. J. Pharm.* 342, 152–160.
- Becke, A.D., 1988. Density-functional exchange-energy approximation with correct asymptotic behavior. *Phys. Rev. A* 38, 3098–3100.
- Becke, A.D., 1993. Density-functional thermochemistry. III. The role of exact exchange. *J. Chem. Phys.* 98, 5648–5652.
- Blaton, N.M., Peeters, O.M., De Ranter, C.J., 1978. The crystal and molecular structure of trans-tetrakis(miconazole)cobalt(II) nitrate. *Acta Cryst.* B34, 1854–1857.
- Dewar, M.J.S., Zoebisch, E.G., Healy, E.F., Stewart, J.J.P., 1985. AM1: a new general purpose quantum mechanical molecular model. *J. Am. Chem. Soc.* 107, 3902–3909.
- Loftsson, T., Brewster, M.E., 1996. Pharmaceutical applications of cyclodextrins. 1. Drug solubilization and stabilization. *J. Pharm. Sci.* 85, 1017–1025.
- Frisch, M.J., Trucks, G.W., Schlegel, H.B., Scuseria, G.E., Robb, M.A., Cheeseman, J.R., Zakrzewski, V.G., Montgomery, J.A., Stratmann, R.E., Burant, J.C., Dapprich, S., Millam, J.M., Daniels, A.D., Kudin, K.N., Strain, M.C., Chen, W., Farkas, O., Tomasi, J., Barone, V., Cossi, M., Cammi, R., Mennucci, B., Pomelli, C., Adamo, C., Clifford, S., Ochterski, J., Petersson, G.A., Ayala, P.Y., Cui, Q., Morokuma, K., Malick, D.K., Rabuck, A.D., Raghavachari, K., Foresman, J.B., Ciolowski, J., Ortiz, J.V., Baboul, A.G.G.,

- Stefanov, B.B., Liu, G., Liashenko, A., Piskorz, P., Komaromi, I., Gomperts, R., Martin, R.L., Fox, D.J., Keith, T., Al-Laham, M.A., Peng, C.Y., Nanyakkara, A., Gonzalez, C., Challacombe, M., Gill, P.M.W., Johnson, B., Wong, M.W., Andres, J.L., Head-Gordon, M., Replogle, E.S., Pople, J.A., 1998. Gaussian 98, A.7. Gaussian, Inc., Pittsburgh PA.
- Frömming, K.H., Szejtli, J., 1994. Cyclodextrins in Pharmacy. Kluwer Academic Publishers, Dordrecht.
- Fu, A., Du, D., Zhou, Z., 2003. Density functional theory study of vibrational spectra of acridine and phenazine. *Spectrosc. Acta Pt A-Molec. Biomolec. Spectr.* 59, 245–253.
- Giese, B., McNaughton, D., 2002. Density functional theoretical (DFT) and surface-enhanced Raman spectroscopic study of guanine and its alkylated derivatives. Part 1. DFT calculations on neutral, protonated and deprotonated guanine. *Phys. Chem. Chem. Phys.* 4, 5161–5170.
- Gorelsky, S.I., 2005. SWizard program. [4.1]. Stanford University, Stanford.
- Johnson, B.G., Gill, P.M.W., Pople, J.A., 1993. The performance of a family of density functional methods. *J. Chem. Phys.* 98, 5612–5626.
- Lee, C., Yang, W., Parr, R.G., 1988. Development of the Colle-Salvetti correlation-energy formula into a functional of the electron density. *Phys. Rev. B* 37, 785–789.
- Piel, G., Dive, G., Evrard, B., Van Hees, T., Henry de Hassonville, S., Delattre, L., 2001a. Molecular modeling study of β - and γ -cyclodextrin complexes with miconazole. *Eur. J. Pharm. Sci.* 13, 271–279.
- Piel, G., Llabres, G., Evrard, B., Van Hees, T., Henry de Hassonville, S., Delattre, L., 2001b. A nuclear magnetic resonance study of the miconazole- β -cyclodextrin inclusion complex in an acidic medium: determination of the structure and stability constants. *STP Pharma Sci.* 11, 235–238.
- Schaftenaar, G., Noordik, J.H., 2000. Molden: a pre- and post-processing program for molecular and electronic structures. *J. Comput. Aid Mod. Des.* 14, 123–134.
- Scott, A.P., Radom, L., 1996. Harmonic vibrational frequencies: an evaluation of Hartree-Fock, Moller-Plesset, quadratic configuration interaction, density functional theory, and semiempirical scale factors. *J. Phys. Chem. A* 100, 16502–16513.
- Wong, M.W., 1996. Vibrational frequency prediction using density functional theory. *Chem. Phys. Lett.* 256, 391–399.